Surrogate ratio method in the actinide region using the $(\alpha, \alpha' f)$ reaction

S. R. Lesher,[1,2,*] J. T. Harke,[1] L. A. Bernstein,[1] H. Ai,[3] C. W. Beausang,[2] D. L. Bleuel,[1,4] R. M. Clark,[4] F. S. Dietrich,[1] J. E. Escher,[1] P. Fallon,[4] J. Gibelin,[4] B. L. Goldblum,[1,5] I. Y. Lee,[4] A. O. Macchiavelli,[4] M. A. McMahan,[4] K. J. Moody,[1] E. B. Norman,[1,4,5] L. Phair,[4] E. Rodriguez-Vieitez,[4] N. D. Scielzo,[1] and M. Wiedeking[1,4]

[1]*Lawrence Livermore National Laboratory, Livermore, California 94551, USA*

[2]*Department of Physics, University of Richmond, Richmond, Virginia 23173, USA*

[3]*Wright Nuclear Structure Laboratory, Yale University, New Haven, Connecticut 06520, USA*

[4]*Lawrence Berkeley National Laboratory, Berkeley, California 94720, USA*

[5]*Department of Nuclear Engineering, University of California, Berkeley, California 94720, USA*

(Received 10 September 2008; revised manuscript received 9 March 2009; published 29 April 2009)

In the Surrogate Method, the measured decay probability of a compound nucleus formed via a direct reaction is used to extract the cross section for a reaction with a different entrance channel that proceeds through the same compound nucleus. An extension of the Surrogate Method, the Surrogate Ratio Method (SRM), uses a ratio of measured decay probabilities to infer an unknown cross section relative to a known one. To test the SRM we compare the direct-reaction-induced fission probability ratio of ^{234}U$(\alpha, \alpha' f)$ to ^{236}U$(\alpha, \alpha' f)$ with the ratio of cross sections of ^{233}U(n, f) to ^{235}U(n, f). These ratios were found to be in agreement over an equivalent neutron energy range of 0.4–18 MeV.

DOI: 10.1103/PhysRevC.79.044609 PACS number(s): 24.10.−i, 24.75.+i, 24.87.+y, 25.85.Ge

I. INTRODUCTION

Neutron-induced reaction cross sections play a role in many areas of nuclear physics and astrophysics, such as nucleosynthesis [1,2], stockpile stewardship, and nuclear energy research [3]. The direct measurement of neutron-induced cross sections can be a challenge, especially with difficult to obtain or short-lived targets. The Surrogate Method, first used by Cramer and Britt in 1970 [4] and more recently by Petit *et al.* [5] and Plettner *et al.* [6] to infer (n, f) cross sections, is based on the assumption that a direct reaction can be used to form a compound nucleus and, therefore, the exit channel is independent of the entrance channel. The (n, f) cross section, $\sigma(n, f)$, can be inferred using the assumption that the decay of the compound nucleus is independent of the angular momentum and parity of the populated states (the Weisskopf-Ewing limit of Hauser-Feshbach theory [7,8]) or that a similar distribution of compound states is excited in the neutron capture and surrogate direct reactions. The cross section is then

$$\sigma(n, f)(E) = \sigma_n^{\mathrm{CN}}(E) P_{\delta f}^{\mathrm{CN}}(E), \tag{1}$$

where σ_n^{CN} is the cross section for forming the compound nucleus via the neutron-induced reaction and $P_{\delta f}^{\mathrm{CN}}$ is the fission probability for the compound nucleus formed via the direct reaction entrance channel δ. E is the excitation energy of the compound nucleus and is the sum of the neutron separation energy (S_n) and the neutron energy (E_n), $E = S_n + E_n$. σ_n^{CN} can be calculated with the help of an appropriate optical-model potential [9] and is typically known more accurately than the decay probabilities $\mathrm{P}_{\delta f}^{\mathrm{CN}}$. Assuming the decay of the compound nucleus is independent of the entrance channel [10], the decay probabilities can be experimentally determined by

$$P_{\delta f}^{\mathrm{CN}}(E) = \frac{N_{\delta f}(E)}{\epsilon_f N_\delta(E)}, \tag{2}$$

where $N_{\delta f}$ is the number of measured particle-fission coincident events, ϵ_f is the efficiency of the fission detector, and N_δ is the total number of observed direct reaction events that form the compound nucleus of interest. By substitution, Eq. (1) becomes

$$\sigma(n, f)(E) = \sigma_n^{\mathrm{CN}}(E) \frac{N_{\delta f}(E)}{\epsilon_f N_\delta(E)}. \tag{3}$$

However, N_δ is often difficult to measure because of backgrounds from the target backings or contaminants.

The Surrogate Ratio Method (SRM) was introduced [6] to overcome the problem with contaminants and create a more model-independent measurement. The validity of this method can be tested by comparing the ratio of fission channel decay probabilities for two similar compound nuclei formed via the same direct reaction to the ratio of two known (n, f) cross sections.

Using Eq. (3), the ratio of $\sigma(n, f)(E)$ for two isotopes (denoted 1 and 2) is expressed as

$$\frac{\sigma_1(n, f)(E)}{\sigma_2(n, f)(E)} = \frac{\sigma_{n1}^{\mathrm{CN}}(E)}{\sigma_{n2}^{\mathrm{CN}}(E)} \times \frac{\epsilon_{f2} N_{\delta 1 f}(E)}{\epsilon_{f1} N_{\delta 2 f}(E)} \times \frac{N_{\delta 2}(E)}{N_{\delta 1}(E)}. \tag{4}$$

The number of direct reaction events is given by

$$N_{\delta i}(E) = \rho_{Ti} \times Q_i \times \epsilon_{\delta i} \times \ell_{ti} \times \sigma_{\delta i}(E), \tag{5}$$

where, for experiment i, the areal target thickness is ρ_T, charge delivered to the target is Q (determined by integrating the beam current), the particle detector efficiency is ϵ_δ, the live time

*lesher1@llnl.gov

fraction is ℓ_t, and the direct reaction cross section integrated over the detector solid angle is σ_δ.

The ratio of the number of direct reaction events is then

$$\frac{N_{\delta 2}(E)}{N_{\delta 1}(E)} = \frac{\rho_{T2}}{\rho_{T1}} \times \frac{Q_2}{Q_1} \times \frac{\epsilon_{\delta 2}}{\epsilon_{\delta 1}} \times \frac{\ell_{t2}}{\ell_{t1}} \times \frac{\sigma_{\delta 2}(E)}{\sigma_{\delta 1}(E)}. \quad (6)$$

The quantity $\sigma_{\delta i}(E)$ is unknown for each reaction individually but, because the same direct reaction on similar target nuclei forms similar compound nuclei, $\sigma_{\delta 2}(E)/\sigma_{\delta 1}(E) \approx 1$ and $\sigma^{\rm CN}_{n1}(E)/\sigma^{\rm CN}_{n2}(E) \approx 1$. If the particle detector geometry is identical, the ratio of the efficiencies $\epsilon_{\delta 2}(E)/\epsilon_{\delta 1}(E) = 1$. Equation (4) becomes

$$\frac{\sigma_1(n,f)}{\sigma_2(n,f)} = \frac{\epsilon_{f2} N_{\delta 1 f}(E)}{\epsilon_{f1} N_{\delta 2 f}(E)} \times \frac{\rho_{T2}}{\rho_{T1}} \times \frac{I_2}{I_1} \times \frac{\Delta t_2}{\Delta t_1} \times \frac{\ell_{t2}}{\ell_{t1}}. \quad (7)$$

Recently, Plettner *et al.* [6] tested the SRM by comparing the fission probability ratios of ^{236}U and ^{238}U formed using the (d, p) reaction to the ratio of the well-known ^{236}U(n, f) and ^{238}U(n, f) cross sections. The two ratios were shown to agree over an excitation energy range of 10 to 22 MeV. In addition, the ratios of fission probabilities $P^{^{238}\rm U}_{(d,d'f)}/P^{^{236}\rm U}_{(d,d'f)}$ were compared to a theoretical model of the $\sigma[^{237}$U$(n, f)]/\sigma[^{235}$U$(n, f)]$ cross-section ratio. Although promising, this result suffered from statistical uncertainties of $\geqslant$20%.

Harke *et al.* [11] used a 55-MeV α beam to perform the direct reactions ^{236}U$(\alpha, \alpha' f)$ and ^{238}U$(\alpha, \alpha' f)$ to improve on the ^{237}U(n, f) cross-section results from Plettner *et al.* [6]. The experimentally measured direct-reaction-induced fission probability ratio was multiplied by the well-known ^{235}U(n, f) cross section to determine the ^{237}U(n, f) cross section in the equivalent neutron energy range of 0–20 MeV with an uncertainty of less than 10%. However, in that work the technique was not benchmarked.

We present a validation of the SRM to extract (n, f) cross sections in the actinide region using inelastic α-particle scattering on ^{234}U and ^{236}U targets that are surrogates for the known neutron-induced reaction cross sections of ^{233}U and ^{235}U nuclei, respectively. This study covers an excitation energy range of 7.2–24.8 MeV, which corresponds to 0.4–18 MeV equivalent neutron energy. We focus on ^{233}U(n, f) and ^{235}U(n, f) cross sections because they are well known [12] and the compound nuclei ^{234}U* and ^{236}U* have similar nuclear structure [neutron separation energy (S_n), deformation, ground-state spin, etc.]. Furthermore, these nuclei have been the subject of a detailed theoretical investigation of the SRM [8]. The results presented in this article suggest that the SRM can be used to successfully obtain unknown (n, f) cross sections via inelastic α-particle scattering and support the results obtained in Ref. [11].

II. EXPERIMENT

In the present experiment, ^{234}U and ^{236}U targets were bombarded with a 55-MeV α-particle beam from the 88-Inch Cyclotron at Lawrence Berkeley National Laboratory. The targets were alternated throughout the 5-day experiment. Each target was made by electroplating uranium onto a 2.29 mg/cm^2 Ta foil. The targets were α counted to determine thickness and purity. The ^{234}U fission target had an areal density of 253 ± 8 μg/cm^2 and the ^{236}U target consisted of 99.68% ^{236}U and 0.32% ^{234}U with an areal density of 184 ± 5 μg/cm^2. No other activity was observed.

The Silicon Telescope Array for Reaction Studies (STARS) [11] was used to detect scattered α's in coincidence with outgoing fission fragments. The STARS array consisted of three double-sided Micron Semiconductor S2 silicon detectors, each segmented into 48 rings and 16 sectors. Each detector had adjacent rings and sectors bussed together for a total of 24 rings and 8 sectors. The particle telescope consisted of two detectors, a 152 μm ΔE and a 994 μm E detector. The particle telescope was placed 15 mm downstream from the target and covered an angular range of $\theta_{\rm polar} = 36^\circ$–$63^\circ$ with respect to the beam axis. Charged particles (p, d, t, ^{3}He, and ^{4}He) were identified by a particle identification plot (PID) based on the range energy relationship of charged particles in silicon [13], as illustrated in Fig. 1. A degrader foil of 4.44 mg/cm^2 Al was placed between the particle telescope and the target to protect the ΔE detector from damage from fission fragments and δ electrons. In addition, a bias of +300 V was applied to the foil to further reduce the effect of δ electrons produced in the target.

A ^{226}Ra α source was used to calibrate the ΔE and E silicon detectors. The ring data did not provide a reliable

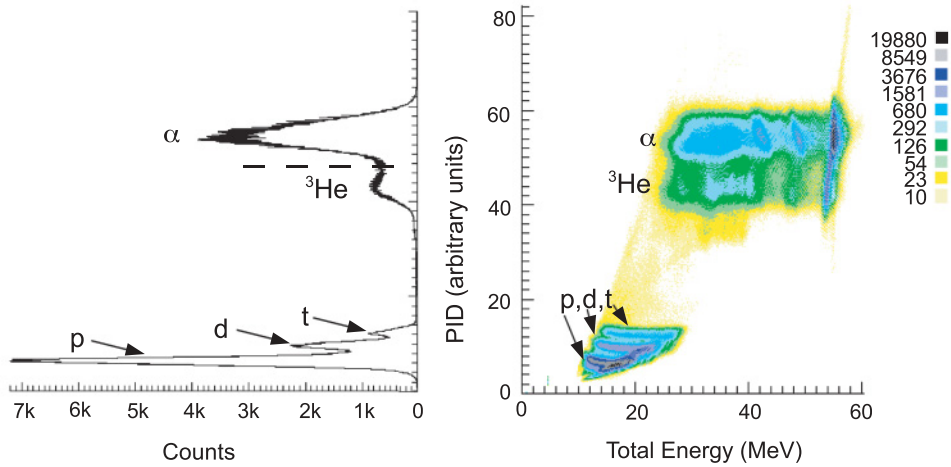

FIG. 1. (Color online) Total energy deposited in the $\Delta E + E$ detectors is plotted versus the particle identification (PID). The PID is defined by $E^{1.80}_{\rm total} - (E_{\rm total} - \Delta E)^{1.80}$. The different charged particles (p, d, t,^{3}He, and ^{4}He) are resolved when the PID plot is projected and the cut (dashed line) differentiates the ^{3}He and ^{4}He particles.

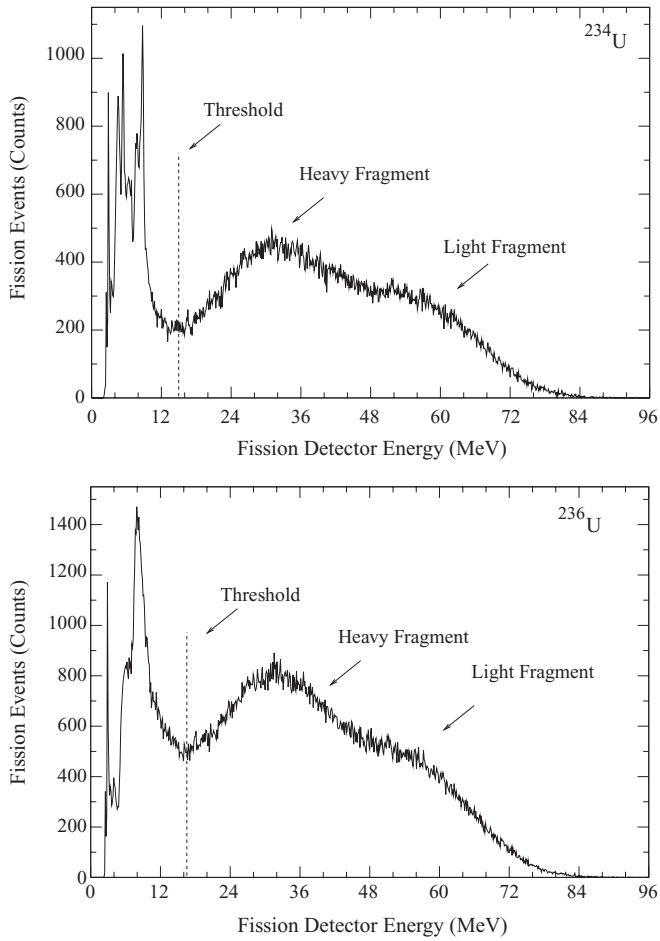

FIG. 2. The measured fission energy spectrum detected in coincidence with α particles for the ^{234}U (top) and ^{236}U (bottom) targets are shown. The fission identification thresholds are noted with a dotted line and differ due to target thickness.

energy measurement because of a small level of cross talk. For this reason, the sector energy was deemed more reliable and used to assign the particle energy. However, the hit ring information was still used to determine the scattering angle for the "ray trace" function (see Sec. III). The 1σ intrinsic detector resolution for a typical sector was 95 and 55 keV in the ΔE and E detectors, respectively.

A third S2 detector, the fission detector, was placed 10 mm upstream from the target to detect fission fragments. This detector covered back angles over an angular range of $\theta_{\text{polar}} = 106^{\circ}$–$132^{\circ}$ with respect to the beam. Figure 2 shows the fission spectrum from the ^{234}U and ^{236}U targets detected in coincidence with α particles. Fission events were identified as having detected energies greater than approximately 15 and 17 MeV for the ^{234}U and ^{236}U fission fragments, respectively, as indicated by the dotted lines in Fig. 2. The fission threshold energies were chosen to account for the different fission fragment energy losses arising from the differing thicknesses of the ^{234}U and ^{236}U targets. The threshold, which roughly corresponds to the maximum energy an α particle can deposit in the detector, effectively excludes events from light charged particles.

The experimental trigger required a coincidence between the ΔE and E detectors. Fission detector energies were recorded if they came within 4 μs of the trigger. The relative time difference between the trigger and the fission detector was recorded using a time-to-amplitude converter (TAC). Prompt particle-fission coincidence events were identified by gating on the peak in the TAC spectrum as shown in Fig. 3. Events outside this gate were considered off-prompt or random particle-fission events.

III. ANALYSIS

The projected range plot, Fig. 1 was used to isolate the ^{4}He particles. A small amount of ^{3}He needed to be subtracted from the ^{4}He data. By fitting each peak with a Gaussian distribution, the amount of ^{3}He in the α peak was estimated to be only $\approx$3% and this correction introduced $<$1% uncertainty in the direct-reaction-induced fission probability ratio.

Each event was "ray traced" from the position in the ΔE and E detectors back to the target plane to ensure that it originated from the target. The polar angle of the scattered particles was determined by the ring that was hit in the ΔE detector and the known distance between the ΔE detector and the target. Particle energies were determined from the sectors of the ΔE and E detectors and corrected for the calculated energy loss in the target, the degrader foil, and the "dead" layers of the silicon detectors. Excitation energies were determined by the difference between the beam energy and the sum of the α-particle energy and the kinematically calculated nuclear recoil energy.

Random events were subtracted from the α-fission coincident data in the following fashion: The random particle-fission events were multiplied by the ratio of the prompt time gate versus the random particle-fission time gate. This yield was then subtracted from the prompt α-fission coincident event data.

The number of α-fission coincident events as a function of equivalent neutron energy for each target is shown in Fig. 4. The number of α-fission coincident events increases at $E_n \approx 0$, 7, and 15 MeV and corresponds to first, second, and third chance fission. At $E_n \gtrsim 18$ MeV, the α particles were stopped in the ΔE detector and did not trigger the data acquisition system (DAQ). Particles above this energy were not analyzed. To compare this data to the (n, f) data, all the quantities in Eq. (7) must be determined.

The areal densities (ρ_τ) of the targets were measured as previously described. The beam current was continuously measured with a Faraday cup to determine Q. The live time fraction (ℓ_t) was measured from the ratio of received triggers to the number of digitized events written to disk and was typically between 60 and 70%.

At energies within a few MeV of the onset of fission, fission fragments from nuclei populated in a direct reaction were preferentially emitted in the plane defined by the scattered particle and recoiling compound nucleus [14]. This anisotropy changes with energy and can lead to a difference in the fission detector efficiency ϵ_{fi} for each target. Because the two nuclei

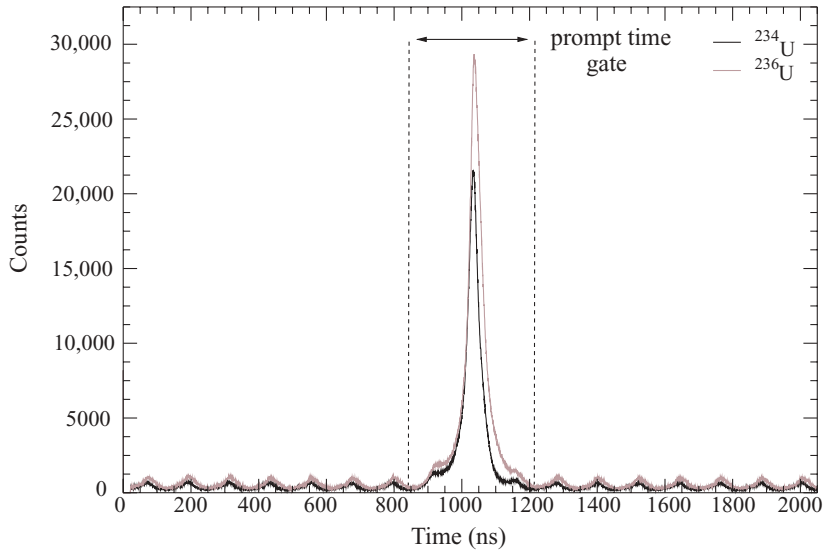

FIG. 3. (Color online) The particle-fission (TAC) spectrum is shown for the ^{236}U data. The dotted lines show the 360 ns gate used to identify prompt particle-fission events. Events outside this gate are considered random events. The periodic structure of the random particle-fission events was due to the 8.26 MHz cyclotron frequency.

populated in this experiment are similar and use the same direct reaction, the anisotropies were expected to be similar. To check this assumption, the number of "in-plane" fission hits was divided by the number of "out-of-plane" fission hits. In-plane fission events were defined as α particles in the same sector in the ΔE detector as fission events in the fission detector and its 180° complement. Fission particles detected in the fission detector sectors at 90° with respect to the plane of the scattered α particle were defined as out-of-plane fission events. This number of in-plane hits divided by the number of out-of-plane hits for both experiments is shown in Fig. 5(a) as a function of excitation energy. Although there is a clear energy dependence for both nuclei, the ratio is unity within experimental errors as shown in Fig. 5(b).

The ratio of the $P^{^{234}\mathrm{U}}_{(\alpha,\alpha' f)}(E_n^{^{233}\mathrm{U}})/P^{^{236}\mathrm{U}}_{(\alpha,\alpha' f)}(E_n^{^{235}\mathrm{U}})$ fission probabilities [as defined in Eq. (2)] was compared with the $\sigma[^{233}\mathrm{U}(n,f)](E_n^{^{233}\mathrm{U}})/\sigma[^{235}\mathrm{U}(n,f)](E_n^{^{235}\mathrm{U}})$ cross section ratio from ENDF-BVII [12] for neutron energies of 0.4–18 MeV in Fig. 6. Where $E_n^{^{233}\mathrm{U}} = E - S_n^{^{234}\mathrm{U}}$ and $E_n^{^{235}\mathrm{U}} = E - S_n^{^{236}\mathrm{U}}$. The data below 0.4 MeV are not used in this comparison because they would include events from below zero neutron energies.

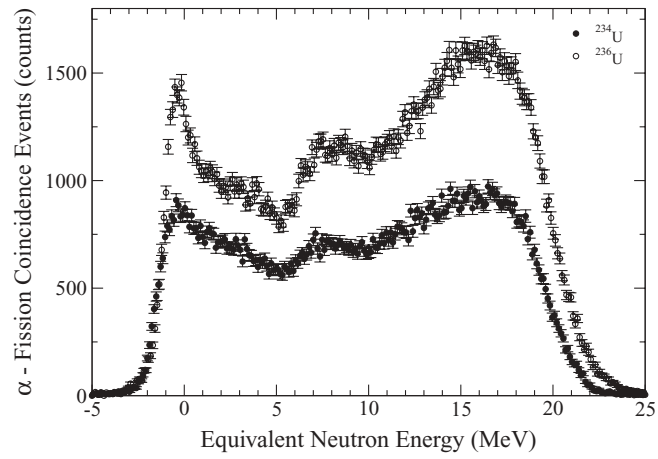

FIG. 4. The background subtracted number of α-fission coincident events as a function of equivalent neutron energy is shown for $^{234}\mathrm{U}(\alpha,\alpha' f)$ (solid circles) and for $^{236}\mathrm{U}(\alpha,\alpha' f)$ (open circles).

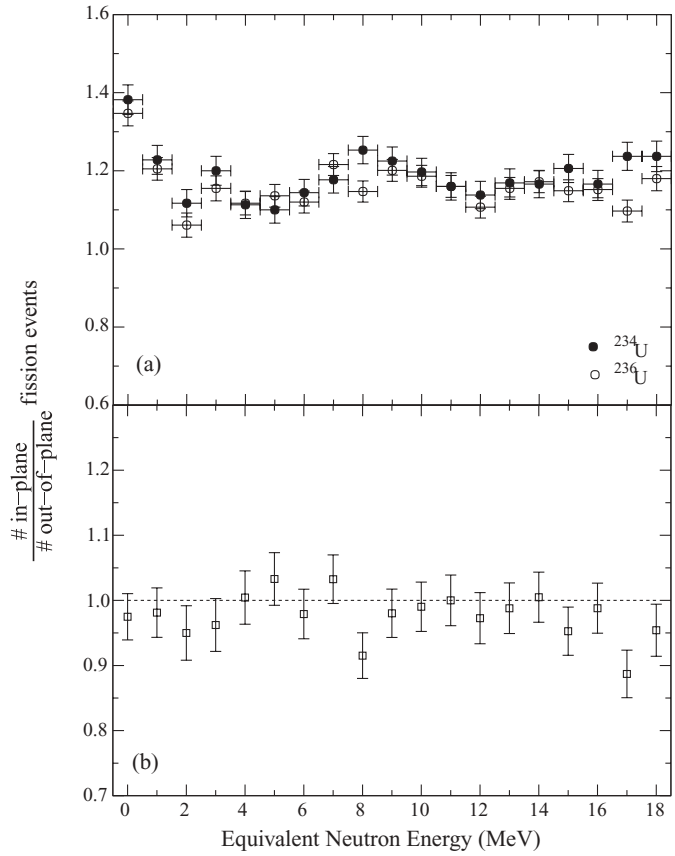

FIG. 5. Part (a) shows the ratio of in-plane versus out-of-plane fission events for ^{234}U and ^{236}U in excitation energy. Although the fission fragments were not emitted isotropically, the ratio for the two nuclei [shown in part (b)] is unity within experimental uncertainties.

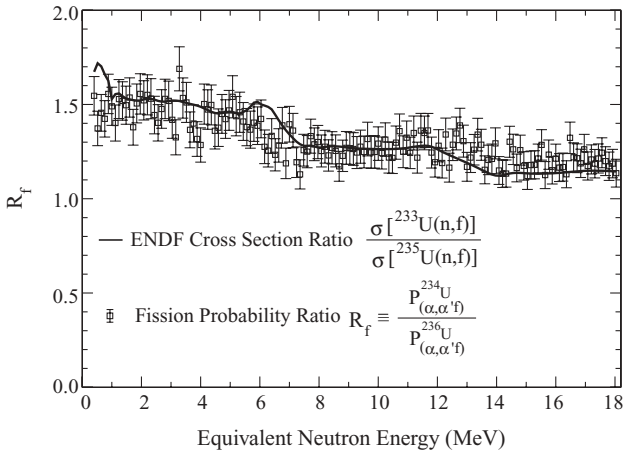

FIG. 6. The direct-reaction-induced fission probability ratio $R_f \equiv P^{234}_{(\alpha,\alpha' f)}/P^{236}_{(\alpha,\alpha' f)}$ fission probability is compared to the $\sigma[^{233}\mathrm{U}(n, f)]/\sigma[^{235}\mathrm{U}(n, f)]$ cross section ratio over an equivalent neutron energy range of 0.4–18 MeV. The energy uncertainty σ for each point has two components, $\sigma = \pm 0.15$ MeV (see Table II) and an energy-dependent component ($\pm 0.02 \times E$) due to the uncertainty in the energy calibration.

The uncertainties in the $P^{234}_{(\alpha,\alpha' f)}(E_n^{233}\mathrm{U})/P^{236}_{(\alpha,\alpha' f)}(E_n^{235}\mathrm{U})$ ratio are shown in Fig. 6 and summarized in Table I. An uncertainty of 4.2% arises from the target thicknesses. The statistical uncertainty varies between 3 and 5% over the excitation energy range of 0.4 and 18 MeV. The sensitivity of the fission identification threshold was tested. This threshold was varied by ±2 MeV and the fission probability ratio was compared to the ratio using the original fission thresholds. A 2.2% systematic uncertainty arises from the choice of the fission fragment energy threshold. The combination of all uncertainties results in a total of 5.6–6.9% over the range of interest.

The energy uncertainties are similar to those discussed in detail in Ref. [11]. The sources of uncertainty arise from energy straggle, angular resolution, intrinsic detector energy resolution, and uncertainty in the beam energy spread (Table II). The energy straggle of the α particles in the degrader foil and target was 47–65 keV and the energy uncertainty caused by the angle of the scattered particle ranged from 25 to 32 keV. Using a ^{226}Ra α source, the 1σ intrinsic detector energy resolution of the telescope was found to range between 102 and 134 keV. The beam energy spread was estimated to be

TABLE I. A summary of the 1σ uncertainties for the $P^{234}_{(\alpha,\alpha' f)}/P^{236}_{(\alpha,\alpha' f)}$ direct-reaction-induced fission probability ratio.

Affected parameter	Source of uncertainty	Relative uncertainty (%)
N_α^{234}	^{234}U target thickness	3
N_α^{236}	^{236}U target thickness	3
$N_{\alpha f}$	Fission spectrum threshold	2.2
$N_{\alpha f}$	Statistical uncertainty	3–5
Total uncertainty		5.6–6.9

TABLE II. A summary of the sources of systematic energy uncertainty quoted in 1σ.

Source	ΔE (keV)
α energy straggle (degrader foil & target)	47–65
Recoil angle uncertainty	25–32
Detector energy resolution (sectors)	102–134
Cyclotron beam	60
Total uncertainty	130–164

±60 keV [11]. The resulting energy uncertainty was $\sigma =$ 130–164 keV.

The highest-energy α from the ^{226}Ra calibration source is 7.6 MeV and the calibration was extrapolated to determine energies up to 55 MeV. This extrapolation gave an elastic peak energy of 55.0 ± 0.5 MeV that agreed with the known beam energy of 55 ± 1 MeV. This agreement verified that such an extrapolation was reasonable and an uncertainty of 2% was assigned to the excitation energy scale.

IV. DISCUSSION

Previous articles [6,11] used the SRM to measure a previously unknown (n, f) cross section. In this article, we verify the validity of this method. The agreement between the α-induced fission probability ratio and the neutron-induced fission cross-section ratio (shown in Fig. 6) provides evidence that a compound nucleus is formed in both types of reactions and that the assumptions underlying the use of the SRM are at least approximately satisfied for the case under consideration. To quantify the agreement between the measured $P^{234}_{(\alpha,\alpha' f)}(E_n^{233}\mathrm{U})/P^{236}_{(\alpha,\alpha' f)}(E_n^{235}\mathrm{U})$ direct reaction-induced fission probability ratio and the accepted $\sigma[^{233}\mathrm{U}(n, f)](E_n^{233}\mathrm{U})/\sigma[^{235}\mathrm{U}(n, f)](E_n^{235}\mathrm{U})$ cross-section ratio, a reduced χ^2 (χ_r^2) was calculated resulting in $\chi_r^2 = 1.127$

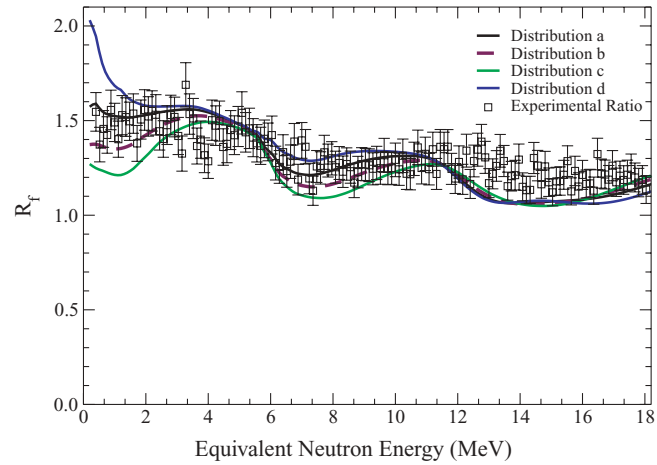

FIG. 7. (Color online) Ratio of fission probabilities $R_f \equiv P^{234}_{(\alpha,\alpha' f)}/P^{236}_{(\alpha,\alpha' f)}$ is plotted (open symbols) as a function of excitation energy. The calculated ratios [8] assume various schematic spin distributions (see Fig. 8) and are given by the indicated lines.

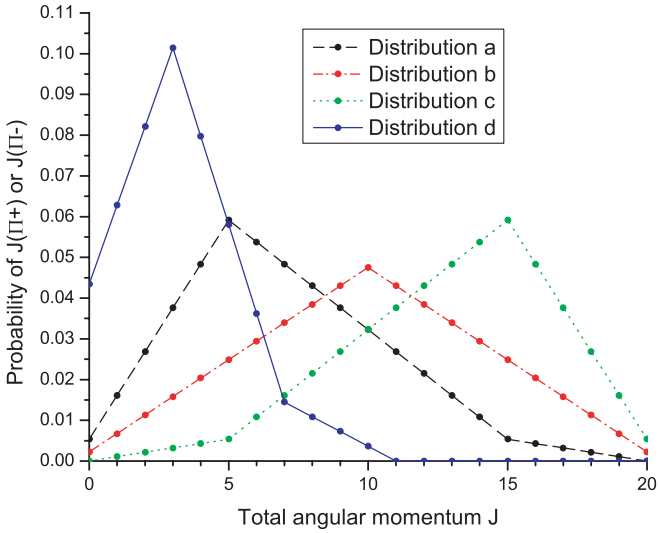

FIG. 8. (Color online) The distributions of total angular momentum are shown for the compound nuclei considered in this study (taken from Ref. [8]). We assume that the $J\pi$ distribution produced in a realistic surrogate reaction falls within the range of the cases shown here. The mean angular momentum is $\langle J\rangle = 7.03$, 10.0, 12.97, and 3.30 for distributions a, b, c, and d, respectively; positive and negative parities are taken to be equally probable.

(for 148 degrees of freedom). The probability of obtaining a larger χ_r^2 is 13.8%. The disagreement between the two data sets at low energies ($E_n < 1$ MeV) is apparent in Fig. 6 and is possibly the result of the Weisskopf-Ewing approximation not being satisfied. Removing these points gives $\chi_r^2 = 0.973$ for 142 degrees of freedom, the probability of obtaining a larger χ_r^2 is 57.5%. This is an acceptable agreement between the ENDF data and the experimental results presented. It should be noted that the ratio method is likely to cancel differences in the direct-reaction-induced fission probability for the two compound nuclei under consideration.

In Fig. 7, the experimentally determined ratio $R_f^{\exp} \equiv P^{234\mathrm{U}}_{(\alpha,\alpha' f)}/P^{236U}_{(\alpha,\alpha' f)}$ is compared to simulated ratios obtained with the model of Ref. [8]. The calculated ratios of fission probabilities (R_f) were obtained as follows: In Ref. [8], Escher and Dietrich carried out a full Hauser-Feshbach calculation of the ^{235}U(n, f) reaction and calibrated the relevant parameters to an evaluation of experimental data. This model was combined with several schematic compound-nuclear spin-parity distributions, $F_\delta^{\mathrm{CN}}(E, J, \pi)$, to simulate decay probabilities $P_{\delta f}^{\mathrm{CN}}(E)$. The simulated fission probabilities thus depend on the spin distribution that was assumed for the decaying compound nucleus ^{236}U*, $P_{\delta f}^{\mathrm{CN}}(E) = P^m[^{236}\mathrm{U}(\alpha, \alpha' f)](E)$, where $m =$ a, b, c, d denotes the J^π distributions shown in Fig. 8. The fission probabilities associated with the decay of ^{234}U* were calculated in an analogous manner; the resulting ratios are shown in Fig. 7.

We observe that the measured data and calculated results are in rough agreement for distributions a, b, and d. Based on insights from previous experiments [15], we expect the $J\pi$ distributions with the smaller average J values, namely, distributions a and d, are more likely to approximate the compound-nuclear spin-parity distribution obtained from inelastic scattering with 55-MeV α particles than the other distributions shown in Fig. 8. The theoretically calculated ratios allow us to identify energy regimes for which the measured fission probability ratio is sensitive to the spin distributions in the decaying compound nuclei, ^{234}U* and ^{236}U*. The largest variations in the theoretically calculated ratios occur at $E_n \leqslant 3$ MeV. We also observe an increased variation between the calculated ratios near the onset of second-chance fission. Both can be expected given the findings summarized in Ref. [8]. Above $E_n \approx 11$ MeV, there is little variation in the theoretically calculated ratios. Possible deviations of the extracted cross section from the expected cross section in that energy range would most likely be due to effects other than a mismatch between the compound-nuclear spin-parity distributions in the desired and surrogate reactions.

V. CONCLUSION

The direct-reaction-induced fission probability ratio, $P^{234\mathrm{U}}_{(\alpha,\alpha' f)}(E_n^{233\mathrm{U}})/P^{236\mathrm{U}}_{(\alpha,\alpha' f)}(E_n^{235\mathrm{U}})$, was compared with the $\sigma[^{233}\mathrm{U}(n, f)](E_n^{233\mathrm{U}})/\sigma[^{235}\mathrm{U}(n, f)](E_n^{235\mathrm{U}})$ cross-section ratio from ENDF-BVII [12] between excitation energies of 0.4 and 18 MeV. This result provides validation of the Surrogate Ratio Method (SRM) for the (α, α') reaction in the even-even actinides.

The SRM offers a new method to obtain fission cross sections on short-lived isotopes that can be applied to a wide variety of basic and applied science topics. This work serves as a benchmark for the SRM to deduce (n, f) cross sections on unstable nuclei using inelastic α scattering. However, the applicability of SRM to (n, γ) and (n, xn) has only begun to be determined. Studies are under way to test the SRM in other mass regions with various direct reactions [16–19].

ACKNOWLEDGMENTS

We thank the 88-Inch Cyclotron operations and facilities staff for their help in performing this experiment. This work was performed under the auspices of the US Department of Energy by Lawrence Livermore National Laboratory in part under Contract W-7405-Eng-48 and in part under Contract DE-AC52-07NA27344 and Grants DE-FG52-06NA26206 and DE-FG02-05ER41379. This work was also supported by the Director, Office of Science, Office of Nuclear Physics of the U.S. Department of Energy under Contract DE-AC02-05CH11231.

[1] S. Goriely and M. Arnould, Astron. Astrophys. **379**, 1113 (2001).

[2] G. J. Wasserburg, M. Busso, R. Gallino, and K. M. Nollett, Nucl. Phys. **A777**, 5 (2006).

[3] International Atomic Energy Agency (Editor), *Fission Product Yield Data for the Transmutation of Minor Actinide Nuclear Waste* (IAEA, Vienna, 2008).
[4] J. D. Cramer and H. C. Britt, Nucl. Sci. Eng. **41**, 177 (1970).
[5] M. Petit, M. Aiche, G. Barreau, S. Boyer, N. Carjan, S. Czajkowski, D. Dassié, C. Grosejean, A. Guiral, B. Haas *et al.*, Nucl. Phys. **A735**, 345 (2004).
[6] C. Plettner, H. Ai, C. W. Beausang, L. A. Bernstein, L. Ahle, H. Amro, M. Babilon, J. T. Harke, J. A. Caggiano, R. F. Casten *et al.*, Phys. Rev. C **71**, 051602(R) (2005).
[7] V. F. Weisskopf and D. H. Ewing, Phys. Rev. **57**, 472 (1940).
[8] J. E. Escher and F. S. Dietrich, Phys. Rev. C **74**, 054601 (2006).
[9] C. A. Bertulani and P. Danielewicz, *Introduction to Nuclear Reactions* (Taylor & Francis, London, 2004).
[10] N. Bohr, Nature (London) **137**, 344 (1936).
[11] J. T. Harke, L. A. Bernstein, J. Escher, L. Ahle, J. A. Church, F. S. Dietrich, K. J. Moody, E. B. Norman, L. Phair, P. Fallon *et al.*, Phys. Rev. C **73**, 054604 (2006).
[12] M. Chadwick, P. Obložinský, M. Herman, N. M. Greene, R. D. McKnight, D. L. Smith, P. G. Young, R. F. MacFarlane, G. M. Hale, S. C. Frankle *et al.*, Nucl. Data Sheets **107**, 2931 (2006).
[13] P. S. Fisher and D. K. Scott, Nucl. Instrum. Methods **49**, 301 (1967).
[14] R. Vandenbosch and J. R. Huizenga, *Nuclear Fission* (Academic Press, New York, 1973).
[15] B. F. Lyles, L. A. Bernstein, J. T. Harke, F. S. Dietrich, J. Escher, I. Thompson, D. L. Bleuel, R. M. Clark, P. Fallon *et al.*, Phys. Rev. C **76**, 014606 (2007).
[16] R. Hatarik, L. A. Bernstein, J. T. Burke, J. A. Cizewski, J. D. Gibelin, S. R. Lesher, P. D. O'Malley, L. W. Phair, and T. Swan, in *Compound-Nuclear Reactions and Related Topics*, edited by J. Escher, F. Dietrich, T. Kawano, and I. J. Thompson, AIP Conf. Proc. (AIP, Melville, NY, 2008), Vol. 1005, p. 105.
[17] N. D. Scielzo, L. A. Bernstein, D. L. Bleuel, J. T. Burke, S. R. Lesher, E. B. Norman, S. A. Sheets, M. S. Basunia, R. M. Clark, P. Fallon *et al.*, in *Compound-Nuclear Reactions and Related Topics*, edited by J. Escher, F. Dietrich, T. Kawano, and I. J. Thompson, AIP Conf. Proc. (AIP, Melville, NY, 2008), Vol. 1005, p. 109.
[18] B. K. Nayak, A. Saxena, D. C. Biswas, E. T. Mirgule, B. V. John, S. Santra, R. P. Vind, R. K. Choudhury, and S. Ganesan, Phys. Rev. C **78**, 061602(R) (2008).
[19] B. L. Goldblum, S. G. Prussin, U. Agvaanluvsan, L. A. Bernstein, D. L. Bleuel, W. Younes, and M. Guttormsen, Phys. Rev. C **78**, 064606 (2008).